Formation of oxide films for high-capacitance aluminum electrolytic capacitor by liquid phase deposition and anodizing

Masatoshi. Sakairi[1)], Ryota Fujita[2)], and Shinji Nagata[3)]

[1)]Faculty of Engineering, Hokkaido University, Kita-13, Nishi-8, Kita-ku, Sapporo, 060-8628, Japan

[2)]Graduate School of Engineering, Hokkaido University, Kita-13, Nishi-8, Kita-ku, Sapporo, 060-8628, Japan
(Presently; Frukawa Electric CO. LTD., 601-2, Otorizawa, Nikko, 321-2336, Japan)

3) Institute for Materials Research, Tohoku University, Katahira-2-1-1, Aoba-ku, Sendai, 980-8577, Japan

Abstract

Liquid phase deposition (LPD) treatment and anodizing were used to form oxide layer for a high-capacitance aluminum electrolytic capacitor. Formation of protective oxide layers and modification of LPD conditions make it possible to prolong the LPD duration and lead to the formation of TiO_2 and NaF deposits on aluminum. A titanium oxide / aluminum oxide mixed layer was formed by a combination process of LPD treatment and anodizing. The capacitance of the formed layer was about 300% higher than that of an anodic oxide film formed on electropolished aluminum. The structures and compositions of the films that were formed were determined by transmission electron microscopy, scanning electron microscopy, and Rutherford backscattering spectroscopy.

Keywords: dielectric film, liquid phase deposition, anodizing, aluminum, titanium oxide.

Introduction

Capacitors such as an aluminum electrolytic capacitor are indispensable components in electrical equipment. Due to the demand for reduction in size and weight of electronic devices, small and high-capacitance capacitors have been required. One of the authors studied incorporation of silicon, niobium or zirconium oxides into anodic oxide films on aluminum to increase specific dielectric constants[1-9]. The electric capacitance achieved was less than 200% of that of an anodic oxide film formed on aluminum without coating. Sol-gel or metal-oxide chemical vapor deposition techniques were used in previous studies for formation of thin oxide films. These techniques have been used for the formation of thin and compact oxide layers on materials. However, the chemicals used in these techniques are costly and require dry conditions during storage and film formation processes. Therefore, a simple technique for the formation of form oxide layers is needed.

One simpler technique is liquid phase deposition (LPD) treatment. LPD treatment is a new surface coating technique for the formation of metal oxide films by dipping the substrate in an aqueous solution[10]. This technique can be used for the formation of metal oxide films on many kinds of substrates. Deki et al. reported fabrication of TiO_2 nanostructures with diameters ranging from 120 to 1065 nm on Si wafers with LPD and electron lithography[11]. Huang et al. reported formation of a self-cleaning and antireflection TiO_2 film on silicon for silicon-based solar cells[12]. The formed film had low water contact angle around 4˚ and the average reflectance of TiO_2/Si structure was 5.3%. Mizuhata et al. reported that formation of TiO_2/porous Si nonocomposites for lithium ion battery by LPD with anodizing[13, 14]. The formed TiO_2/porous Si showed high charge/discharge capacity without rapid degradation. Wu et at. reported formation of an $SrTiO_3$ film on an AlGN/GaN wafer for gate dielectric in a metal oxide semiconductor high electron mobility transistor (MOSHEMT)[15]. Lei et al. reported a dense and crack-free anatase TiO_2 film with thickness of 800 nm was formed by LPD at 353K for 10.8 ks on ITO conducting grass as photo-anodes for cathodic protection of SUS 304 stainless steel[16]. Lee et al. reported fabrication of photocatalytic TiO_2 films on stainless steel by LPD at 333 K using TiF_4 and H_3BO_3[17]. The formed TiO_2 films showed a preferential orientation, and formed films showed photocatalytic activity without high-temperature treatment. The formed TiO_2 films exhibited sufficiently negative potential under illumination, and they could serve as the photo anodes for cathodic protection of the steels. Fujita et al. reported formation of corrosion-resistant TiO_2 films on magnesium and the structures and chemical compositions of the films[18,

[19]. The films formed in weak alkaline solution with sucrose showed good corrosion resistance. Sakairi et al. reported fabrication of alumina films with nano-dot structures by successive liquid phase deposition, anodizing, and substrate dissolution[20]. They suggested that a continuous supply of suitable amounts of F^- and H^+ ions to the specimen surface was important to form the alumina film with nano-dot structures.

In this study, formation of titanium oxide / aluminum oxide mixed layers on pre-anodized aluminum was attempted by using LPD and post-anodizing. The structure and dielectric properties of oxide films formed on aluminum were examined.

Experimental

Specimens

Highly pure aluminum sheets (99.99 mass%, 25 mm×15 mm×0.1 mm) was used as specimens. The specimens were electropolished at a constant voltage of 28 V and at 281 K for 150 s. The electropolished solution used was a mixture of 13.6 kmol m^{-3} CH_3COOH (Kanto Chemical Co. Ltd., 99.7 mass%) / 2.56 kmol m^{-3} $HClO_4$ (Kanto Chemical Co. Ltd., 60 mass%).

Protective oxide layer formation

As suggested film formation reactions in the literature[10, 14], the concentrations of F^- and H^+ ions on the specimen surface can be increased even if boric acid (H_3BO_3) is added to the solution to remove these ions. Due to the presence of these harmful ions, the aluminum substrate is easily dissolved when dipped in the LPD solution. Therefore, some protective films are required for the formation of TiO_2 film on the aluminum substrate. Crystalline oxide films formed by heat treatment and anodizing were used as protective oxide layers.

The electropolished specimens were ultrasonically cleaned in ethanol (Kanto Chemical Co. Ltd., 99.5 mass%) for 600 s. After cleaning, the specimens were heat-treated at 823 K for 10.8 ks in air and then anodized at a constant current density of 5 $mAcm^{-2}$ up to 100 V in 0.5 kmol m^{-3} H_3BO_3 (Kanto Chemical Co. Ltd., 99.5 mass%) / 0.05 kmol m^{-3} $Na_2B_4O_7$ (Kanto Chemical Co. Ltd., 98.0 mass%) at 353 K.

Liquid phase deposition (LPD) and re-anodizing

Specimens with protective oxide layers were immersed in 0.05 kmol m^{-3} ammonium hexafluorotitanate ($(NH_4)_2TiF_6$) (Sigma Aldrich Inc., 99.99 mass%) / 0.2 kmol m^{-3} H_3BO_3 (Kanto Chemical Co. Ltd., 99.5 mass%) with 0.2 kmol m^{-3} sucrose (Kanto

Chemical Co. Ltd., guaranteed reagent) from t_L = 0.9 ks to 7.2 ks at 353 K. The pH of the solutions was adjusted with sodium hydroxide (NaOH) (Kanto Chemical Co. Ltd., 97.0 mass%). Sucrose acts an inhibitor for TiO_2 excess homogeneous nucleation in LPD solutions. LPD-treated specimens were re-anodized at a constant current density of 1 $mAcm^{-2}$ up to 100 V in 0.5 kmol m^{-3} H_3BO_3 / 0.05 kmol m^{-3} $Na_2B_4O_7$ at 293 K.

Characterization of the formed films

Electrochemical impedance were measured by using a frequency response analyzer (FRA, NF Corporation, S-5720B) and a sine wave of 100 mV was used.

Specimen surfaces after treatment were examined by using a scanning electron microscope (SEM, JEOL Ltd., JSM-6510LA) equipped with an energy dispersive X-ray spectroscope (EDS). Cross sections of the LPD specimens were examined by using a transmission electron microscope (TEM, JEOL Ltd., JEM-2000FX) equipped with an EDS. The oxide films were also analyzed by Rutherford backscattering spectroscopy (RBS, High Voltage Engineering Tandetron) using a 2.0 MeV He^{2+} ion beam supplied by a Van de Graff accelerator. The He^{2+} ion beam angle was normal to the specimen surface, and the detector angle was 170 degrees to the incident direction. The chemical compositions and thicknesses of the films that were formed were determined using the RUMP program.

Results and discussion

Re-anodizing behavior of LPD-treated specimens

Figure 1 shows changes in cell voltage, E_{ra}, during re-anodizing after LPD treatment for t_L=3.6 ks at different value of pH. The curve for a specimen that has been electropolished and anodized in a re-anodizing condition (Electro-polished) is also shown for comparison. The curve for the specimen treated by LPD at pH 11.5 is almost the same as that for the Electro-polished one, and the curve for the specimen treated at pH 8.0 is steeper than that at pH 11.5. The curve for the specimen treated by LPD at pH 3.8 is different from that of other specimens. It shows almost no increase of E_{ra} at the initial and then shows a jump and sudden increase around 215 s. The results for the pH 11.5 specimen indicate that the protective oxide layer may dissolve during LPD treatment and that the surface area and initial surface conditions are almost the same as those of the Electro-polished specimen. A jump of about 5 V in E_{ra} is observed in the LPD-treated at pH 8.0 specimen, and the curve then steeply increases compared to the curves for the Electro-polished and pH 11.5 specimens. These results suggest that

pre-formed protective oxide films remains after LPD treatment. The film thickness per unit film formation voltage for crystalline anodic oxide film is reported to be 1.30 to 0.90 nm/V[21]. From this ratio and observed initial jump in E_{ra}, the remaining barrier layer thickness is expected to about 6 nm.

Figure 2 shows changes in cell voltage during re-anodizing with different value of t_L at pH 8.0. Result for the Electro-polished specimen is shown in the figure as a reference. In the figure, t_L=0 s indicates without LPD treatment, meaning that there is no damaged of the protective oxide layer. Regardless of t_L, the rate of increase in cell voltage (film formation rate) is faster than that for the Electro-polished specimen. The slope of the current for the LPD-treated specimens changes with increase in t_L, indicating that the thickness of the protective oxide layer or deposited layer is changed with increase in t_L.

Electrochemical impedance behavior

Figure 3 shows a Bode diagram for specimens re-anodizing after LPD treatment at (a) t_L=3.6 ks with different value of pH and (b) different value of t_L at pH 8.0. As a reference for LPD treatment, results for the Electro-polished specimen are also shown in all graphs of Figure 3. The log |Z| vs. log *f* curve for all specimens shows a straight line with a slope of about -1 in the frequency range from 10 to 10^4 s^{-1} with a horizontal straight line above 10^4 s^{-1}. Phase shift shows about -90º in the frequency range from 10 to 10^3 s^{-1}, and it increases with changes of frequency in both low and high frequency ranges.

The previously reported simple equivalent electric circuit[1-5] can be applied to calculate capacitance of the films that were formed. Figure 4 shows changes in capacitance of the films obtained from Figure 3 as a function of (a) pH and (b) t_L. As can be seen in figure 4 (a), capacitance shows a maximum at pH 8.0. Figure 4 (b) shows that the capacitance increases with longer t_L. The capacitance of the LPD specimen treated at pH 8.0 and t_L=7.2 ks is about 300% higher than that of the Electro-polished specimen. From the present study, the best condition for formation of high capacitance films is LPD solution pH of 8.0 and LPD duration of 7.2 ks. However, further study is required to determine the optimum conditions for formation of more higher capacitance films.

Structure and composition of the film

Figure 5 shows RBS spectra of LPD-treated specimens at different value of pH and t_L. right row figures are expanded around 300 channel number of left row figures. From

analysis of the RBS spectra, protective layers (initially formed Al_2O_3 film) with thicknesses of about 200 nm remained after LPD treatment regardless of t_L. Ti-related peaks are observed for all specimens. Analysis of the RBS spectra indicated that a small amount of TiO_2 was deposited on the protective oxide layers in all specimens.

Figure 6 shows TEM cross-sectional images of LPD-treated and re-anodized specimens under different conditions of LPD treatment. Re-anodized oxide films are observed in all conditions of LPD treatment, and no protective oxide layers are observed in acid and alkaline LPD treatments. TiO_2 particles can be seen in Fig. 6 (a). However, regardless of the conditions of LPD treatments, no Ti peak was observed by TEM-EDS inside either the protective oxide layers or re-anodized oxide films.

Figure 7 shows SEM surface images of re-anodized specimens under different conditions of LPD treatment. Because of the resolution of EDS, no Ti peak was observed by EDS analysis for any of the specimens. A rough surface is observed on the LPD-treated specimen at pH 3.6 and t_L=3.6 ks, and powder-like deposits are observed inside the broken area. From EDS analysis, Al and O peaks were observed both inside and outside of broken area. An uneven surface is observed on the LPD-treated specimen at pH 3.6 and t_L=3.6 ks, and Al and O peaks were observed by EDS analysis. NaF deposits are observed on LPD-treated specimens at pH 8.0. The NaF deposits may decrease reliability of the formed films. Therefore, the amount of NaF deposits must be reduced for practical capacitor applications of the films, and further studies are needed to achieve small depositions of NaF.

The surface films formed by LPD treatment and re-anodizing are summarized in Fig. 8 (pH 8.0 for different value of t_L) and in Fig. 9 (t_L=3.6 ks at different value of pH). In the LPD condition of pH 8.0, the protective oxide layers may dissolve locally and form defects, but they remain even after long t_L. Depositions of TiO_2 and NaF also occurs during LPD treatment. TiO_2 and Al_2O_3 mixed layers may form with re-anodizing, and the formation of the films lead to increase capacitance. As shown in Fig. 9, at both high and low pH of LPD treatment, protective oxide layers may be greatly dissolved during LPD treatment. Almost dissolved protective oxide films make it difficult to incorporate the TiO_2 particles into the Al_2O_3 films during re-anodizing.

Conclusions

Liquid phase deposition (LPD) treatment and anodizing were used for the formation of form a titanium oxide/aluminum oxide mixed layer for a high-capacitance aluminum electrolytic capacitor. Optimization of the conditions of LPD treatment and formation of

a protective oxide layer make it possible to prolong the LPD duration and lead to the formation of TiO_2 and NaF deposits on the aluminum. The capacitance of the formed layer under optimized conditions is about 300% higher than that of an anodic oxide film formed on electropolished aluminum. The results also suggest that reduction of the NaF deposition is required for practical capacitor applications.

Acknowledgments

A part of this work is financially supported by The Light Metals Educational Foundation Inc..

Reference

[1] K. Watanabe, M. Sakairi, H. Takahashi, S. Hirai, S. Yamaguchi, *J. Surf. Finish. Soc. Jpn.*, **1999**; 50, 359.

[2] K. Watanabe, M. Sakairi, H. Takahashi, S. Hirai, S. Yamaguchi, *J. Electroanal. Chem.*, **1999**; 473, 250.

[3] K. Watanabe, M. Sakairi, H. Takahashi, K. Takahiro, S. Nagata, S. Hirai, *Electrochemistry*, **1999**; 67, 1243.

[4] K. Watanabe, M. Sakairi, H. Takahashi, K. Takahiro, S. Nagata, S. Hirai, *Electrochemistry*, **2001**; 69, 407.

[5] K. Watanabe, M. Sakairi, H. Takahashi, K. Takahiro, S. Nagata, S. Hirai, *J. Electrochem. Soc.*, **2001**; 148, B473.

[6] S. Koyama, T. Kikuchi, M. Sakairi, H. Takahashi, S. Nagata, *Electrochemistry*, **2007**; 75, 573.

[7] M. Sunada, T. Kikuchi, M. Sakairi, H. Takahashi, S. Hirai, *J. Solid State Elecherochm.*, **2007**; 11, 1375.

[8] L. Yao, J. Liu, M. Yu, S. Li, H. Wu, T*rans. Nonferrous Metals Soc. of China*, **2010**; 20, 825.

[9] X. Du, Y. Xu, *Thin Solid Films*, **2008**; 516, 8436.

[10] S. Deki, Y. Aoi, O. Hiroi, A. Kajinami, *Chem. Lett.*, **1996**; 25, 433.

[11] S. Deki, S. Iizuka, A. Horie, M. Mizuhata, A. Kajinami, *Chem. Mater.*, **2004**; 16, 1747.

[12] J. Huang and Y. Lee, *Surface & coating technology*, **2013**; 231, 257.

[13] M. Mizuhata, A. Katayama, H. Maki, *ECS Trans.*, **2014**; 61, 9.

[14] M. Mizuhata, A. Katayama, H. Maki, *J. Flourine Chem.*, **2015**; 174, 62.

[15] T. Wu, C. Hu, P. Sze, T. Huang, F. Adriyato, C. Wu and Y. Wang, *Solid-State Electronics*, **2013**; 82, 1.
[16] C. X. Lei, H. Zhou, Z. D. Feng, Y. F. Zhu, R. G. Du, *J. Alloy and Compounds*, **2012**; 513, 552.
[17] S. C. Lee, H. Yu, J. Yu, C.H. Ao, *J. Cryst. Growth*, **2006**; 295, 60.
[18] M. Sakairi, R. Fujita, T. Kikuchi, S. Nagata, *Proc. of 5th Int. Sympo. Marine Corros. and Control*, Qingdo, **2011**; 277.
[19] R. Fujita, M. Sakairi, T. Kikuchi, *Electorochim. Acta*, **2011**; 56, 7180.
[20] M. Sakairi, R. Fujita, H. Jha, T. Kikuchi, *Surface and Interface Analysis special Issue of ASST2012*, **2013**; 45, 1510.
[21] H. Takahashi, Y Umehara, T. Miyamoto, N. Fujimoto, M. Nagayama, *J. Surf. Fin. Soc. Jpn.*, **1987**; 38, 66.

Caption list

Fig. 1 Changes in cell voltage, E_{ra}, during re-anodizing after LPD treatment for t_L=3.6 ks at different value of pH.

Fig. 2 Changes in cell voltage during re-anodizing with different t_L at pH 8.0.

Fig. 3 Bode diagram for specimens re-anodizing after LPD treatment at (a) t_L=3.6 ks with different value of pH and (b) different value of t_L at pH 8.0.

Fig. 4 Changes in capacitance of the formed films obtained from Figure 3 as a function of (a) pH and (b) t_L.

Fig. 5 RBS spectra of LPD treated specimens at different pH and t_L.

Fig. 6 TEM cross-sectional images of LPD-treated and re-anodized specimens under different conditions of LPD treatment.

Fig. 7 SEM surface images of LPD treated and re-anodized specimens at different LPD conditions.

Fig. 8 Summary of films formed by LPD and re-anodizing treatments at pH 8.0 for different t_L

Fig. 9 Summary of films formed by LPD and re-anodizing treatments for t_L=3.6 ks at different pH.

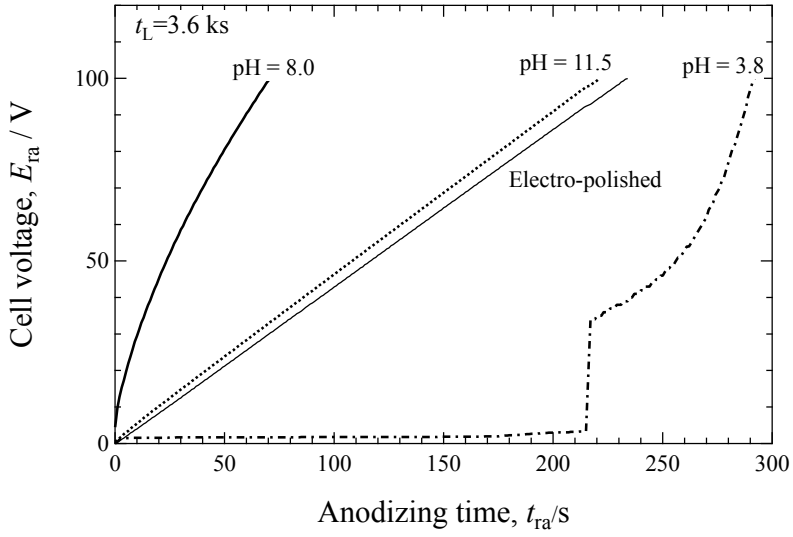

Fig. 1

Sakairi et al.

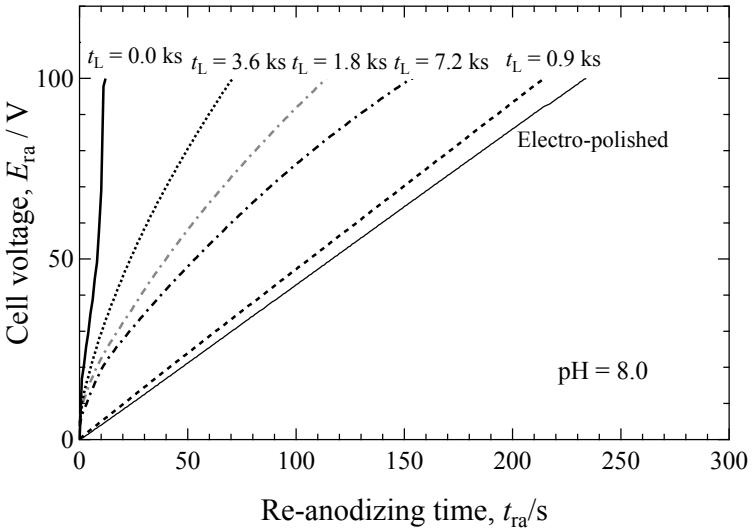

Fig. 2

Sakairi et al.

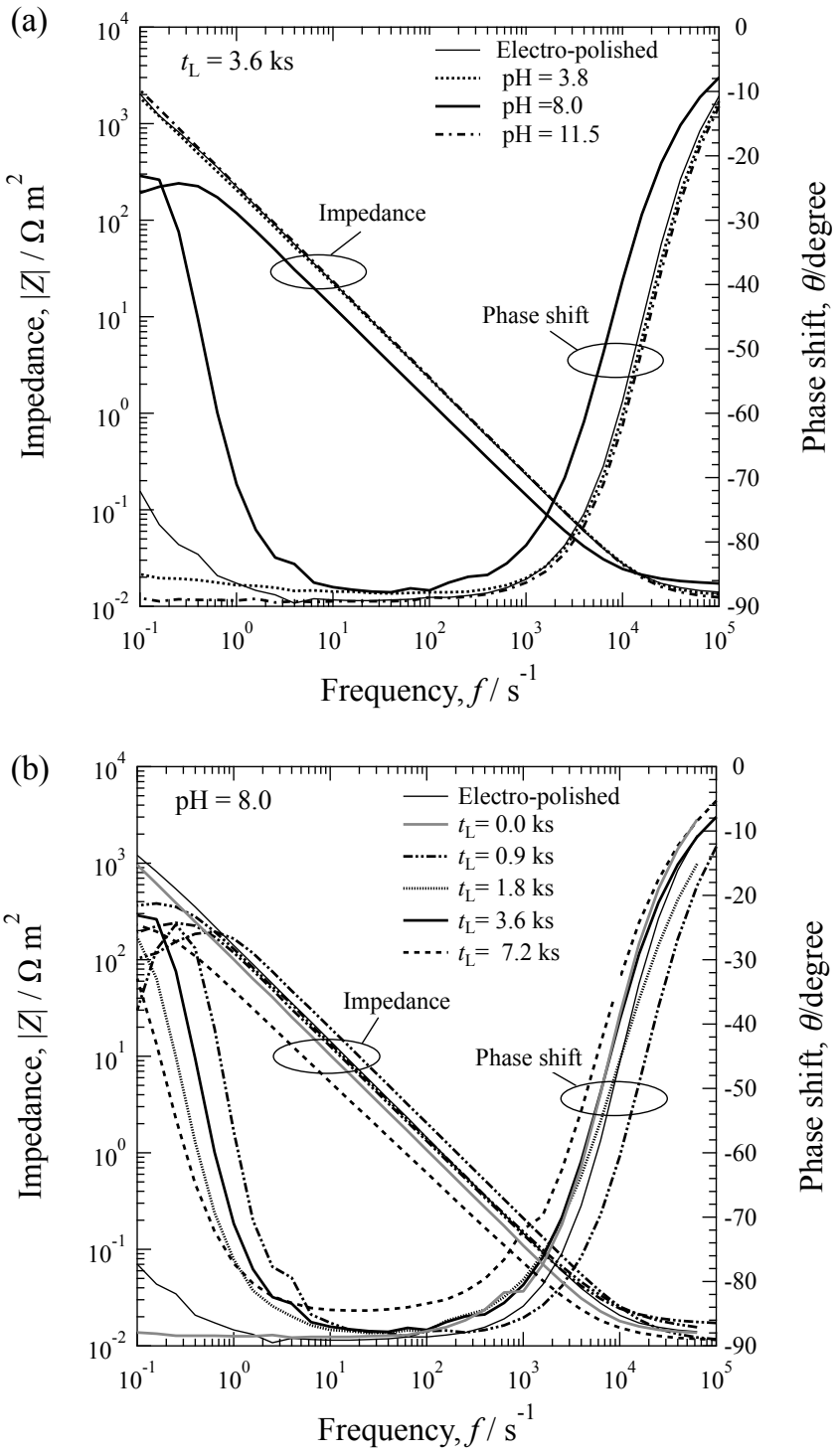

Fig.3

Sakairi et al.

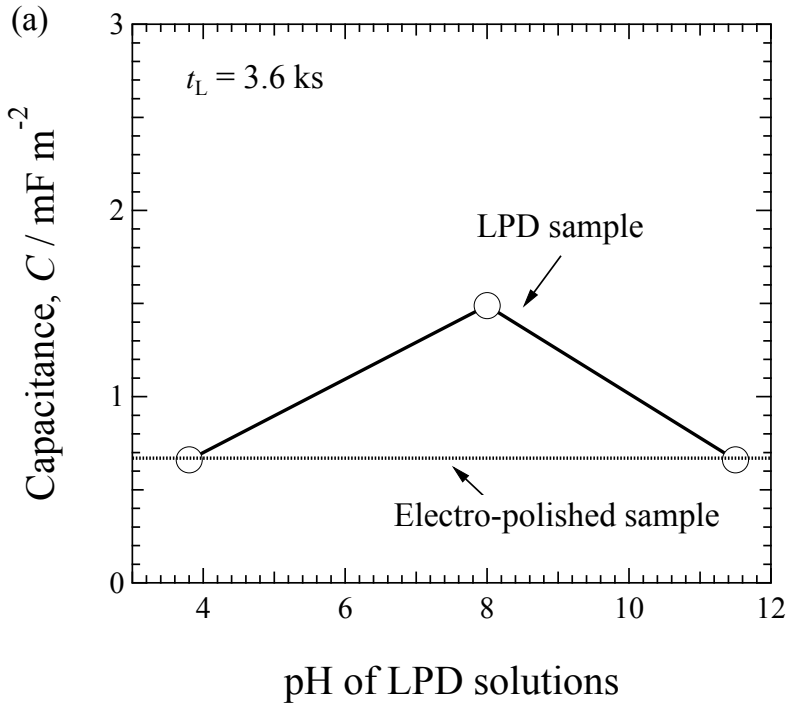

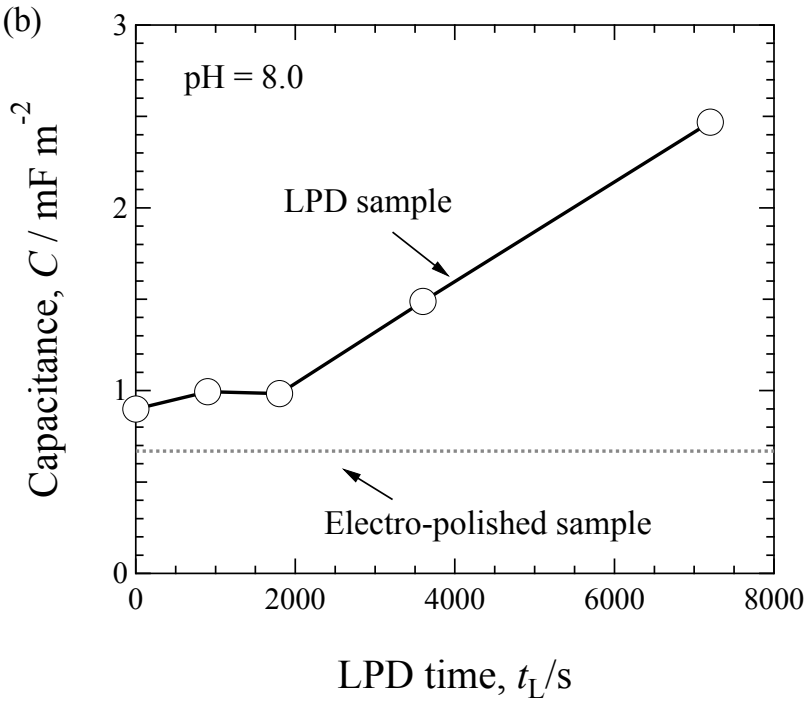

Fig.4

Sakairi et al.

(a) pH = 3.8, t_L = 3.6 ks

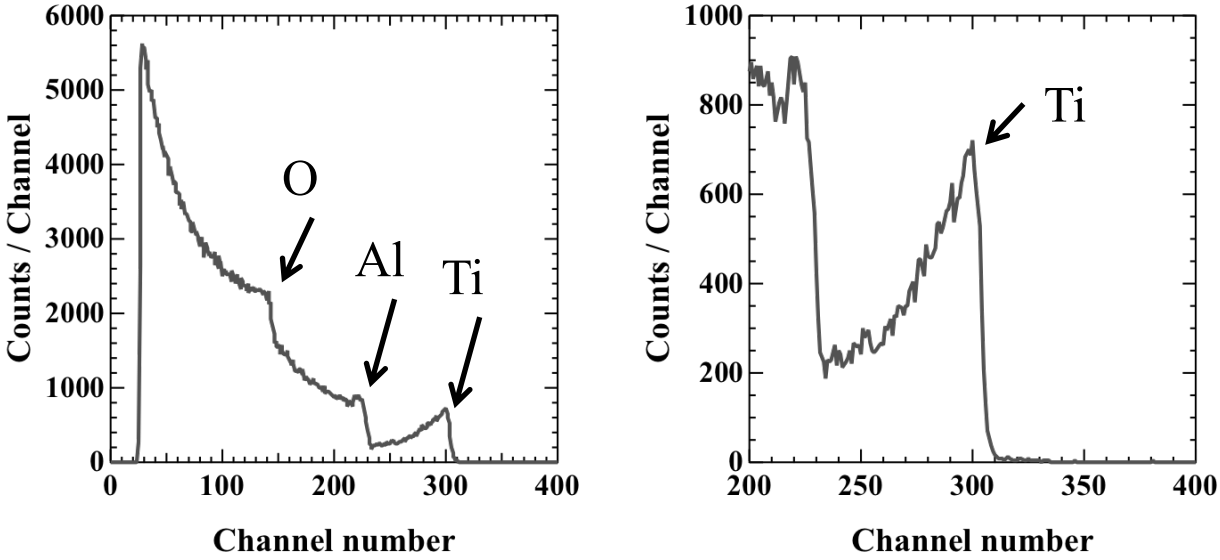

(b) pH = 8.0, t_L = 3.6 ks

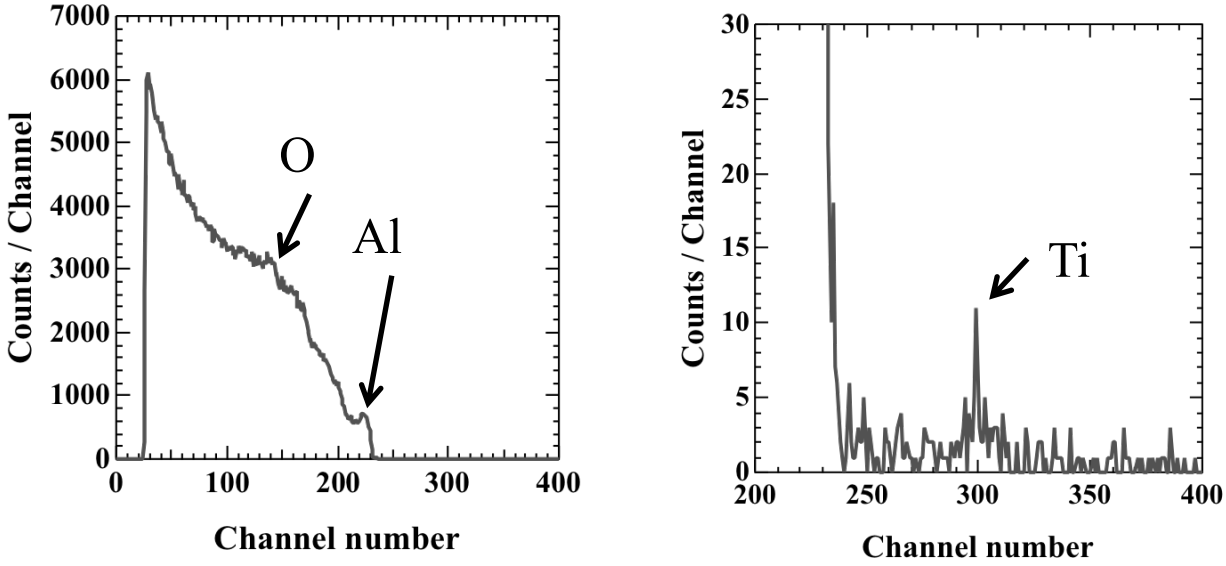

(c) pH = 11.5, t_L = 3.6 ks

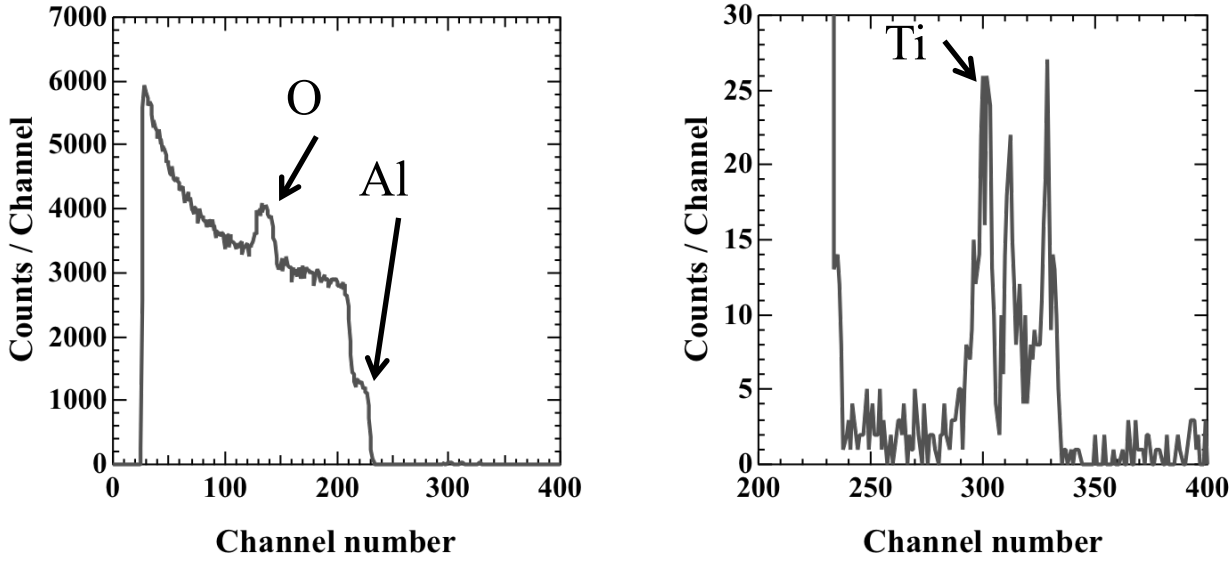

Fig.5

Sakairi et al.

(a) pH = 3.8, t_L = 3.6 ks

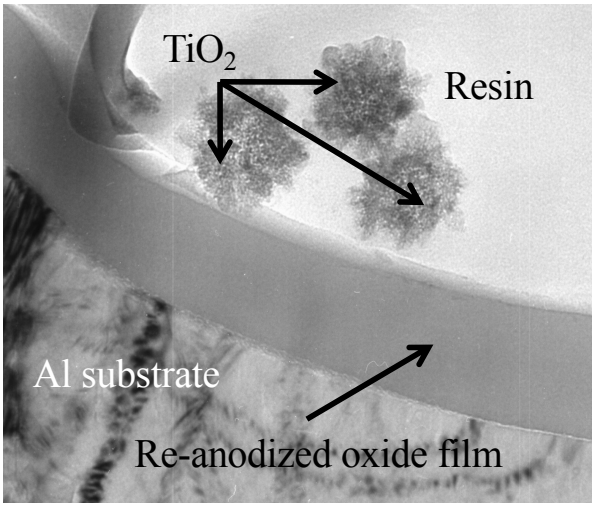

(b) pH = 11.5, t_L = 3.6 ks

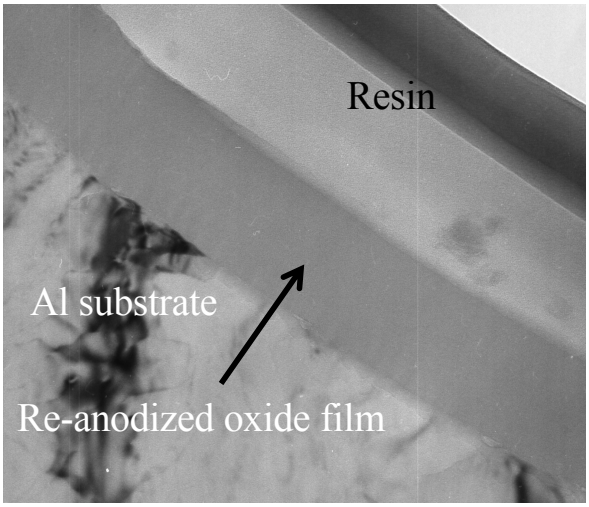

(c) pH = 8.0, t_L = 3.6 ks

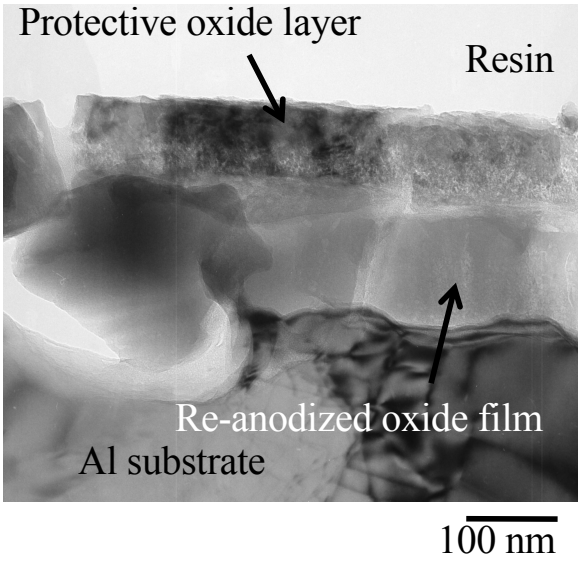

(d) pH = 8.0, t_L = 7.2 ks

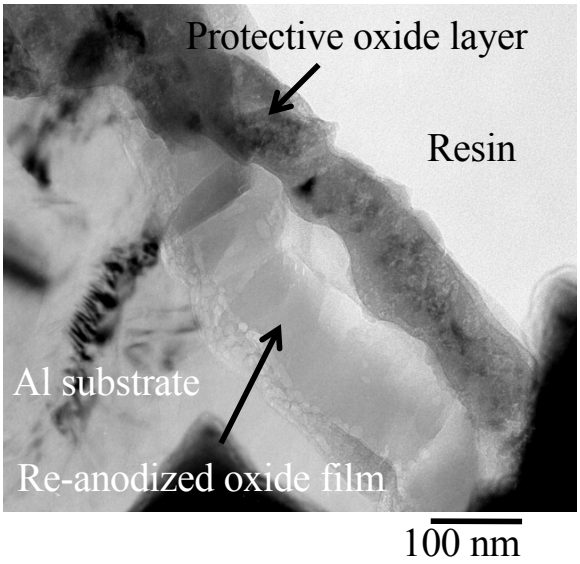

Fig. 6

(a) pH = 3.8, t_L = 3.6 ks

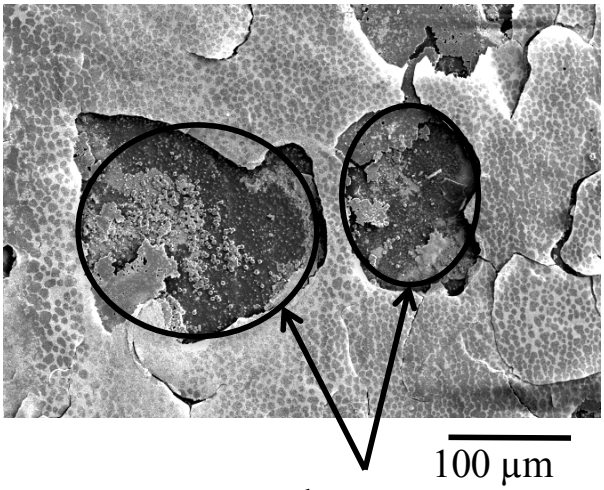

(b) pH = 3.8, t_L = 3.6 ks
(Expansion of (a))

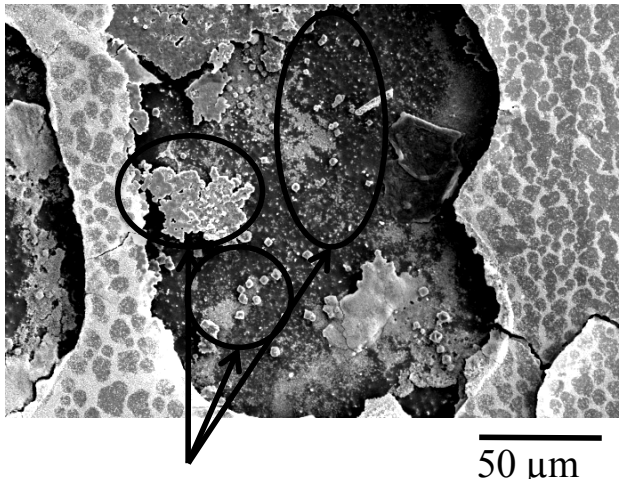

(c) pH = 11.5, t_L = 3.6 ks

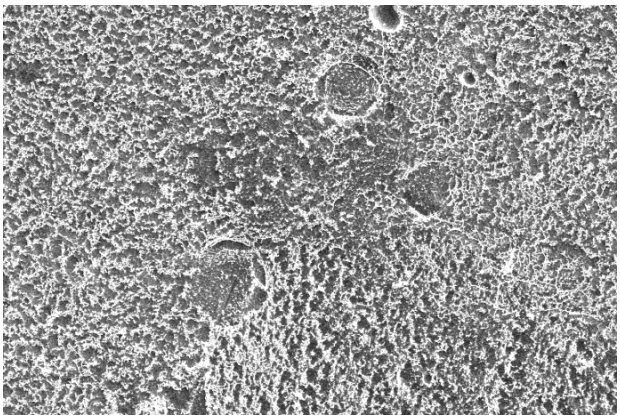

(d) pH = 8.0, t_L = 0.9 ks

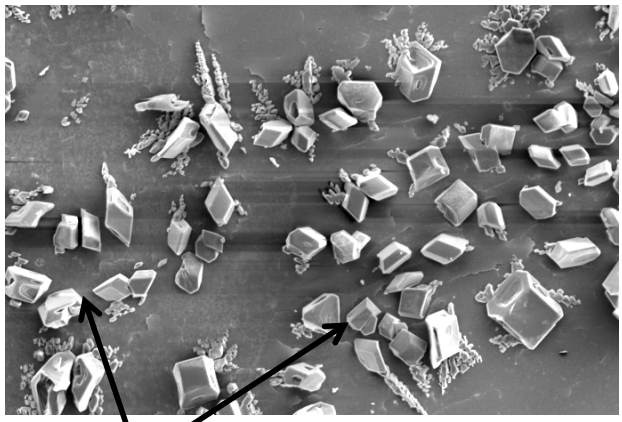

(e) pH = 8.0, t_L = 3.6 ks

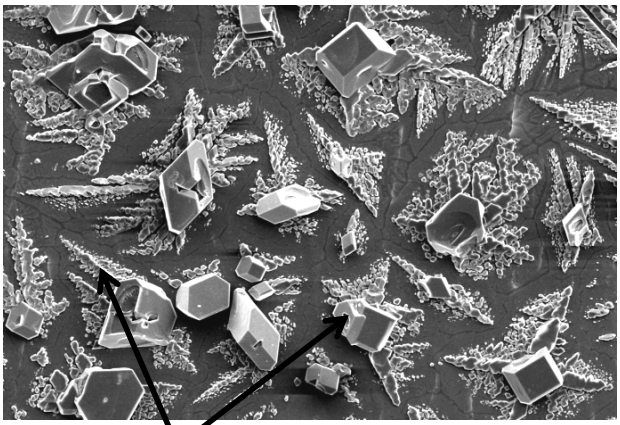

(f) pH = 8.0, t_L = 7.2 ks

Fig.7

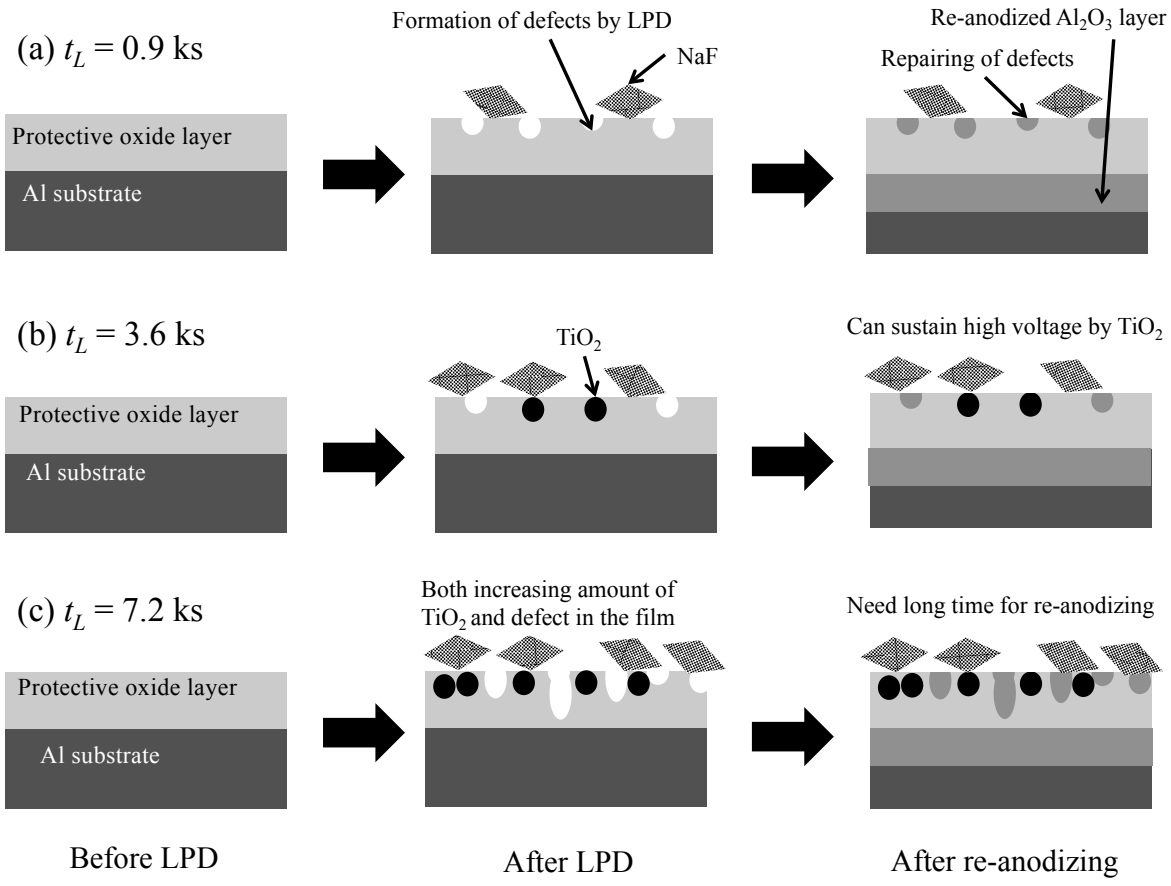

Fig.8

Sakairi et al.

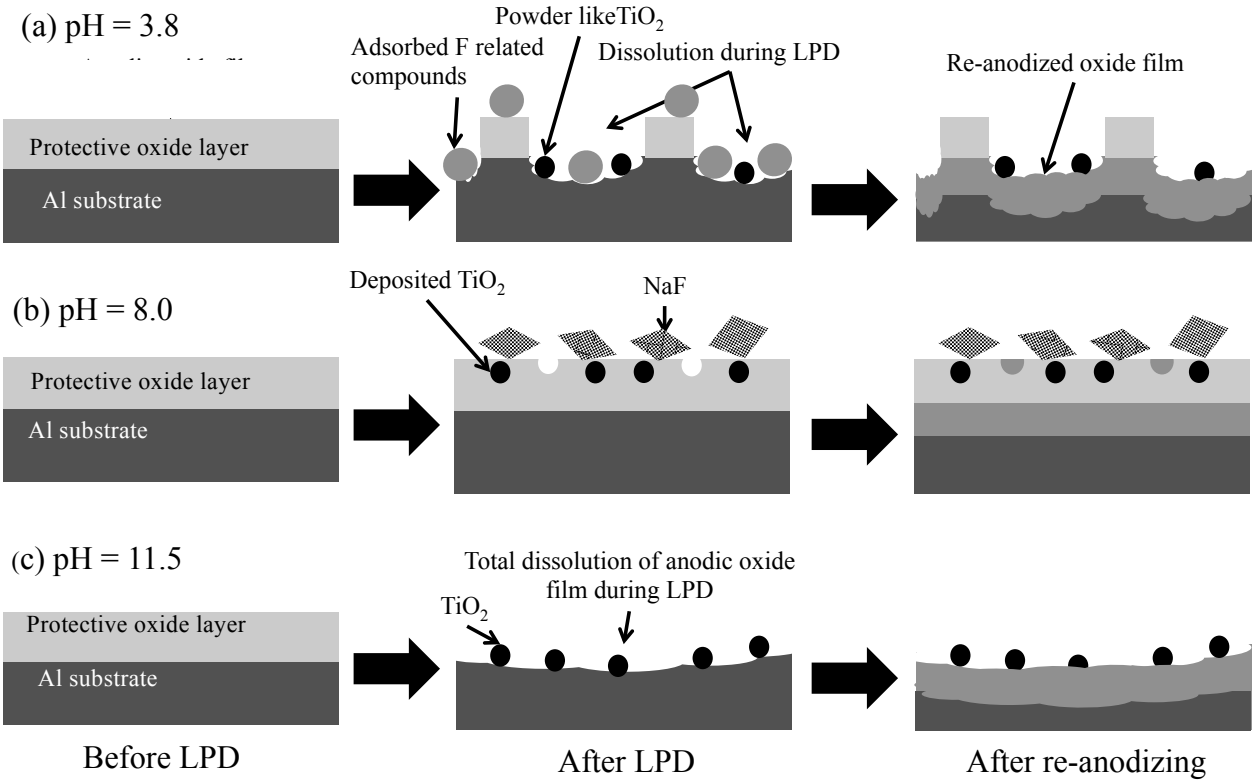

Fig.9

Sakairi et al.